Yoshii and Eto *Nanoscale Research Letters* 2011, **6**:604
http://www.nanoscalereslett.com/content/6/1/604

Nanoscale Research Letters
a SpringerOpen Journal

NANO EXPRESS

Analytical expression of Kondo temperature in quantum dot embedded in Aharonov-Bohm ring

Ryosuke Yoshii* and Mikio Eto

Abstract

We theoretically study the Kondo effect in a quantum dot embedded in an Aharonov-Bohm ring, using the "poor man's" scaling method. Analytical expressions of the Kondo temperature T_K are given as a function of magnetic flux Φ penetrating the ring. In this Kondo problem, there are two characteristic lengths, $L_c = \hbar v_F/|\tilde{\varepsilon}_0|$ and $L_K = \hbar v_F = T_K$, where v_F is the Fermi velocity and $\tilde{\varepsilon}_0$ is the renormalized energy level in the quantum dot. The former is the screening length of the charge fluctuation and the latter is that of the spin fluctuation, i.e., size of Kondo screening cloud. We obtain diferent expressions of $T_K(\Phi)$ for (i) $L_c \ll L_K \ll L$, (ii) $L_c \ll L \ll L_K$, and (iii) $L \ll L_c \ll L_K$, where L is the size of the ring. T_K is remarkably modulated by Φ in cases (ii) and (iii), whereas it hardly depends on Φ in case (i).

PACS numbers:

Introduction

Since the first observation of the Kondo effect in semiconductor quantum dots [1-3], various aspects of Kondo physics have been revealed, owing to the artificial tunability and flexibility of the systems, e.g., an enhanced Kondo effect with an even number of electrons at the spin-singlet-triplet degeneracy [4], the SU(4) Kondo effect with $S = 1/2$ and orbital degeneracy [5], and the bonding and antibonding states between the Kondo resonant levels in coupled quantum dots [6,7]. One of the major issues which still remain unsolved in the Kondo physics is the observation of the Kondo singlet state, so-called Kondo screening cloud. The size of the screening cloud is evaluated as $L_K = \hbar v_F/T_K$, where v_F is the Fermi velocity and T_K is the Kondo temperature. There have been several theoretical works on L_K, e.g., ring-size dependence of the persistent current in an isolated ring with an embedded quantum dot [8], Friedel oscillation around a magnetic impurity in metal [9], and spin-spin correlation function [10,11].

We focus on the Kondo effect in a quantum dot embedded in an Aharonov-Bohm (AB) ring. In this system, the conductance shows an asymmetric resonance as a function of energy level in the quantum dot, so-called Fano-Kondo effect. This is due to the coexistence of one-body interference effect and many-body Kondo effect, which was studied by the equation-of-motion method with the Green function [12], the numerical renormalization group method [13], the Bethe ansatz [14], the density-matrix renormalization group method [15], etc. This Fano-Kondo resonance was observed experimentally [16]. The interference effect on the value of T_K, however, has not been fully understood [17,18].

In our previous work [19], we examined this problem in the small limit of AB ring using the scaling method [20]. Our theoretical method is as follows. First, we create an equivalent model in which a quantum dot is coupled to a single lead. The AB interference effect is involved in the flux-dependent density of states in the lead. Second, the two-stage scaling method is applied to the reduced model, to renormalize the energy level in the quantum dot by taking into account the charge fluctuation and evaluate T_K by taking spin fluctuation [21]. This method yields T_K in an analytical form.

The purpose of this article is to derive an analytical expression of T_K for the finite size of the AB ring, using our theoretical method. We find two characteristic lengths. One is the screening length of the charge fluctuation, $L_c = \hbar v_F/|\tilde{\varepsilon}_0|$ with $\tilde{\varepsilon}_0$ being the renormalized energy level in the quantum dot, which appears in the first stage of the scaling. The other is the size of Kondo screening cloud, L_K, which is naturally obtained in the second stage. In consequence, the analytical expression of T_K is different for situations (i) $L_c \ll L_K \ll L$, (ii) $L_c \ll L \ll L_K$, and (iii) $L \ll L_c \ll L_K$, where L is the size of the ring. We show

* Correspondence: festina.lente@a3.keio.jp
Faculty of Science and Technology, Keio University, 3-14-1 Hiyoshi, Kohoku-ku, Yokohama 223-8522, Japan

that T_K strongly depends on the magnetic flux Φ penetrating the AB ring in cases (ii) and (iii), whereas it hardly depends on Φ in case (i).

Model

Our model is shown in Figure 1a. A quantum dot with an energy level ε_0 is connected to two external leads by tunnel couplings, V_L and V_R. Another arm of the AB ring (reference arm) and external leads are represented by a one-dimensional tight-binding model with transfer integral $-t$ and lattice constant a. The size of the ring is given by $L = (2l + 1)a$. The reference arm includes a tunnel barrier with transmission probability of $T_b = 4x/(1 + x)^2$ with $x = (W/t)^2$. The AB phase is denoted by $\varphi = 2\pi\Phi/\Phi_0$, with flux quantum $\Phi_0 = h/e$. The Hamiltonian is

$$H^{(0)} = H_{\rm dot} + H_{\rm leads + ring} + H_{\rm T}, \tag{1}$$

$$H_{\rm dot} = \sum_{\sigma} \varepsilon_0 d_\sigma^\dagger d_\sigma + U\hat{n}_\uparrow \hat{n}_\downarrow, \tag{2}$$

$$\begin{aligned} H_{\rm leads + ring} = &\sum_{i\neq 0}\sum_{\sigma} (-t a_{i+1,\sigma}^\dagger a_{i,\sigma} + {\rm h.c.}) \\ &+ \sum_{\sigma} (W e^{i\phi} a_{1,\sigma}^\dagger a_{0,\sigma} + {\rm h.c.}), \end{aligned} \tag{3}$$

$$H_{\rm T} = \sum_{\sigma} (V_L d_\sigma^\dagger a_{-l,\sigma} + V_R d_\sigma^\dagger a_{l+1,\sigma} + {\rm h.c.}), \tag{4}$$

where $d_\sigma^\dagger$ and d_σ are creation and annihilation operators, respectively, of an electron in the quantum dot with spin σ. $a_{i,\sigma}^\dagger$ and $a_{i,\sigma}$ are those at site i with spin σ in the leads and the reference arm of the ring. $\hat{n}_\sigma = d_\sigma^\dagger d_\sigma$ is the number operator in the dot with spin σ. U is the charging energy in the dot.

We consider the Coulomb blockade regime with one electron in the dot, $-\varepsilon_0, \varepsilon_0 + U \gg \Gamma$, where $\Gamma = \Gamma_L + \Gamma$ is the level broadening. $\Gamma_\alpha = \pi \nu_0 V_\alpha^2$, with ν_0 being the local density of states at the end of semi-infinite leads. We analyze the vicinity of the electron-hole symmetry of $-\varepsilon_0 \approx \varepsilon_0 + U$.

We create an equivalent model to the Hamiltonian (1), following Ref. [19]. First, we diagonalize the Hamiltonian $H_{\rm leads+ring}$ for the outer region of the quantum dot. There are two eigenstates for a given wavenumber k; $|\psi k,\rightarrow\rangle$ represents an incident wave from the left and partly reflected to the left and partly transmitted to the right, whereas $|\psi_k,\leftarrow\rangle$ represents an incident wave from the right and partly reflected to the right and partly transmitted to the left. Next, we perform a unitary transformation for these eigenstates

$$(|\bar{\psi}_k\rangle \quad |\psi_k\rangle) = (|\psi_{k,\rightarrow}\rangle \quad |\psi_{k,\leftarrow}\rangle) \begin{pmatrix} A_k & B_k^* \\ B_k & -A_k^* \end{pmatrix},$$

where A_k and B_k are determined so that $\langle d|H_{\rm T}|\bar{\psi}_k\rangle = 0$ with dot state $|d\rangle$. In consequence, mode $|\psi_k\rangle$ is coupled to the dot via $H_{\rm T}$, whereas $|\bar{\psi}_k\rangle$ is completely decoupled.

Neglecting the decoupled mode, we obtain the equivalent model in which a quantum dot is coupled to a single lead. In a wide-band limit, the Hamiltonian is written as

$$\begin{aligned} H = &\sum_{\sigma} \varepsilon_0 d_\sigma^\dagger d_\sigma + U\hat{n}_\uparrow \hat{n}_\downarrow + \sum_{k,\sigma} \varepsilon_k a_{k,\sigma}^\dagger a_{k,\sigma} \\ &+ \sum_{k,\sigma} V(d_\sigma^\dagger a_{k,\sigma} + {\rm h.c.}), \end{aligned} \tag{5}$$

with $V = \sqrt{V_L^2 + V_R^2}$ and density of states in the lead

$$\nu(\varepsilon_k) = \nu_0 \left[1 - R_b \cos\frac{\varepsilon_k + D_0}{\varepsilon_T} - P(\phi)\sin\frac{\varepsilon_k + D_0}{\varepsilon_T}\right] \tag{6}$$

Here, D_0 is the half of the band width, k_F is the Fermi wavenumber, $R_b = 1 - T_b$, and

$$P(\phi) = \sqrt{\alpha T_b(1 - T_b)}\cos\phi, \tag{7}$$

where $\alpha = 4\Gamma_L\Gamma_R/(\Gamma_L + \Gamma_R)^2$ is the asymmetric factor for the tunnel couplings of quantum dot.

The AB interference effect is involved in the flux-dependent density of states in the lead, $\upsilon(\varepsilon_k)$ in Eq. (6). As schematically shown in Figure 1(b), $\upsilon(\varepsilon_k)$ oscillates with the period of ε_T, where $\varepsilon_T = \hbar v_F/L$ is the Thouless energy for the ballistic systems. We assume that $\varepsilon_T \ll D_0$.

Scaling analysis

We apply the two-stage scaling method to the reduced model. In the first stage, we consider the charge fluctuation at energies of $D \gg |\varepsilon_0|$. In this region, the number of electrons in the quantum dot is 0, 1, or 2. We reduce the energy scale from bandwidth D_0 to D_1 where the charge fluctuation is quenched. By integrating out the excitations in the energy range of $D_1 < D < D_0$, we renormalize the energy level in the quantum dot ε_0. In the second stage of scaling, we consider the spin fluctuation at low energies of $D < D_1$. We make the Kondo Hamiltonian and evaluate the Kondo temperature.

Renormalization of energy level

In the first stage, the charge fluctuation is taken into account. We denote E_0, E_1, and E_2 for the energies of the empty state, singly occupied state, and doubly occupied state in the quantum dot, respectively. Then the energy levels in the quantum dot are given by $\varepsilon_0 = E_1 - E_0$ for the first electron and $\varepsilon_1 = E_2 - E_1$ for the second electron. When the bandwidth is reduced from D to $D - |{\rm d}D|$, E_0,

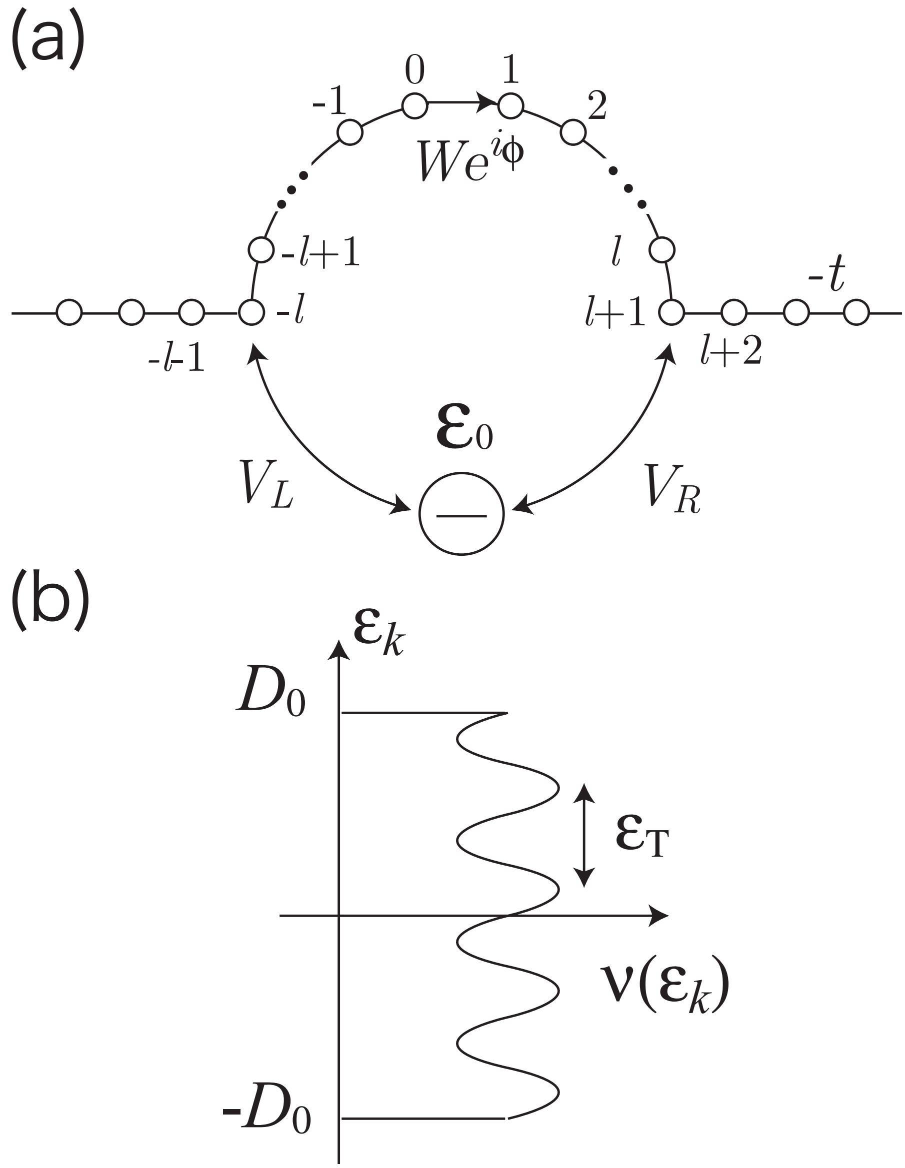

Figure 1 (a) Model for an Aharonov-Bohm (AB) ring with an embedded quantum dot. A quantum dot with an energy level ε_0 is connected to two external leads by tunnel couplings, V_L and V_R. Another arm of the AB ring (reference arm) and external leads are represented by a one-dimensional tight-binding model. The reference arm includes a tunnel barrier with transfer integral W. The magnetic flux Φ penetrating the ring is considered as an AB phase $\varphi = 2\pi\Phi/\Phi_0$ with flux quantum $\Phi_0 = h/e$. **(b)** The density of states in the lead for the reduced model, $\nu(\varepsilon_k)$ in Eq. (6). $\nu(\varepsilon_k)$ oscillates with the period of ε_T, the Thouless energy for the ballistic systems. Its amplitude and phase depend on the AB phase φ.

E_1, and E_2 are renormalized to E_0 + dE_0, E_1 + dE_1, and E_2 + dE_2, where

$$\mathrm{d}E_0 = -\frac{2V^2\nu(-D)}{D+E_1-E_0}|\mathrm{d}D|,$$

$$\mathrm{d}E_1 = -\left[\frac{V^2\nu(D)}{D+E_0-E_1} + \frac{V^2\nu(-D)}{D+E_2-E_1}\right]|\mathrm{d}D|,$$

$$\mathrm{d}E_2 = -\frac{2V^2\nu(D)}{D+E_1-E_2}|\mathrm{d}D|,$$

within the second-order perturbation with respect to tunnel coupling V. For $D \gg |E_1 - E_0|$, $|E_2 - E_1|$, they yield the scaling equations for the energy levels

$$\frac{\mathrm{d}\varepsilon_i}{d\ln D} = 2\nu_0 V^2 f(k_\mathrm{F}L, \phi)\sin\frac{D}{\varepsilon_\mathrm{T}}, \tag{8}$$

where i = 0, 1 and

$$f(k_\mathrm{F}L, \phi) = R_\mathrm{b}\sin k_\mathrm{F}L - P(\phi)\cos k_\mathrm{F}L. \tag{9}$$

By the integration of the scaling equation from D_0 to $D_1 \simeq |\tilde{\varepsilon}_0|$, we renormalize the energy levels in the quantum dot ε_i to $\tilde{\varepsilon}_1$:

$$\tilde{\varepsilon}_i - \varepsilon_i \simeq 2\nu_0 V^2 f(k_F L, \phi)\left[\mathrm{Si}\left(\frac{|\varepsilon_0|}{\varepsilon_T}\right) - \mathrm{Si}\left(\frac{D_0}{\varepsilon_T}\right)\right], \quad (10)$$

where

$$\mathrm{Si}(x) = \int_0^x \frac{\sin\xi}{\xi} d\xi.$$

$\mathrm{Si}(x)$ goes to 0 as $x \to 0$ and $\pi/2$ as $x \to \infty$.

From Equation 10, we conclude that

$$\tilde{\varepsilon}_i \simeq \varepsilon_i - \pi\nu_0 V^2 f(k_F L, \phi), \quad (11)$$

when $\varepsilon_T \gg |\tilde{\varepsilon}_0|$, and $\tilde{\varepsilon}_i = \varepsilon_i$ when $\varepsilon_T \ll |\tilde{\varepsilon}_0|$. These results can be rewritten in terms of length scale. We introduce $L_c = \hbar v_F / |\tilde{\varepsilon}_0|$, which corresponds to the screening length of charge fluctuation. When $L \ll L_c$, the renormalized level $\tilde{\varepsilon}_i$ is given by Equation 11. When $L \gg L_c$, the energy level is hardly renormalized and is independent of φ.

Renormalization of exchange coupling

In the second stage, we consider the spin fluctuation at low energies of $D < D_1$. For the purpose, we make the Kondo Hamiltonian via the Schrieffer-Wolff transformation,

$$H_{\mathrm{Kondo}} = \sum_{k,\sigma} \varepsilon_{k\sigma} a^\dagger_{k\sigma} a_{k\sigma} + H_J + H_K, \quad (12)$$

$$\begin{aligned} H_J = J\sum_{k',k} [&S^+ a^\dagger_{k'\downarrow} a_{k\uparrow} + S^- a^\dagger_{k'\uparrow} a^\dagger_{k\downarrow} \\ &+ S_z(a^\dagger_{k'\uparrow} a_{k\uparrow} - a^\dagger_{k'\downarrow} a_{k\downarrow})], \end{aligned} \quad (13)$$

$$H_k = K\sum_{k',k}\sum_{\sigma} \sigma^\dagger_{k'\sigma} a_{k\sigma}, \quad (14)$$

where $S^+ = d^\dagger_\uparrow d_\downarrow$, $S^- = d^\dagger_\downarrow d_\uparrow$ and $S_z = (d^\dagger_\uparrow d_\uparrow - d^\dagger_\downarrow d_\downarrow)/2$ are the spin operators in the quantum dot. The density of states in the lead is given by Equation 6 and half of the band width is now $D_1 \simeq |\tilde{\varepsilon}_0|$. H_J represents the exchange coupling between spin 1/2 in the dot and spin of conduction electrons, whereas H_K represents the potential scattering of the conduction electrons by the quantum dot. The coupling constants are given by

$$J = V^2\left(\frac{1}{|\tilde{\varepsilon}_0|} + \frac{1}{\tilde{\varepsilon}_1}\right), \quad K = \frac{V^2}{2}\left(\frac{1}{|\tilde{\varepsilon}_0|} - \frac{1}{\tilde{\varepsilon}_1}\right).$$

By changing the bandwidth, we renormalize the coupling constants J and K so as not to change the low-energy physics within the second-order perturbation with respect to H_J and H_K. Then we obtain the scaling equations of

$$\begin{aligned} \frac{dJ}{d\ln D} = &- 2\nu_0 J^2\left[1 - f(k_F L + \pi/2, \varphi)cos\frac{D}{\varepsilon_T}\right] \\ &- 4\nu_0 JKf(k_F L, \varphi)sin\frac{D}{\varepsilon_T}, \end{aligned} \quad (15)$$

$$\frac{dK}{d\ln D} = -2\nu_0\left(\frac{3}{4}J^2 + 4K^2\right)f(k_F L, \varphi)sin\frac{D}{\varepsilon_T}, \quad (16)$$

The energy scale D where the fixed point ($J \to \infty$) is reached yields the Kondo temperature.

Scaling equations (15) and (16) are analyzed in two extreme cases. In the case of $D \gg \varepsilon_T$, the oscillating part of the density of states $\nu(\varepsilon_k)$ is averaged out in the integration [22]. Then the scaling equations are effectively rewritten as

$$\frac{dJ}{d\ln D} \simeq -2\nu_0 J^2, \quad (17)$$

$$\frac{dK}{d\ln D} \simeq 0. \quad (18)$$

In the case of $D \ll \varepsilon_T$, the expansion around the fixed point [23] yields

$$\frac{K}{J} \simeq \frac{3}{8}c, \quad (19)$$

$$2\nu(D)J = \frac{[1 + O(c^2)]}{\ln(1+\xi)}, \quad (20)$$

where $\xi = D/T_K$ - 1 and

$$c \simeq \frac{2f(k_F L, \phi)}{1 - f(k_F L, \phi)}\frac{D}{\varepsilon_T}. \quad (21)$$

Now we evaluate the Kondo temperature in situations (i) $L_c \ll L_K \ll L$, (ii) $L_c \ll L \ll L_K$, and (iii) $L \ll L_c \ll L_K$, where $L_K = v_F\hbar/T_K$. In situation (i), $\varepsilon_T \ll T_K$ and thus J and K follow Equations 17 and 18 until the scaling ends at $D \simeq T_K$. Integration of Equation 17 from D_1 to T_K yields

$$T_K \simeq |\varepsilon_0| \exp(-1/2\nu_0 J) \equiv T_K^{(0)}, \quad (22)$$

where $J = V^2(|\varepsilon_0|^{-1} + \varepsilon_1^{-1})$.

In situation (iii), $D_1 \ll \varepsilon_T$. Then the scaling equations (19) and (20) are valid in the whole scaling region ($T_K < D < D_1$). From the equations, we obtain

$$T_K(\phi) \simeq |\varepsilon_0|\left(T_K^{(0)}/|\varepsilon_0|\right)^{f(\phi)}, \quad (23)$$

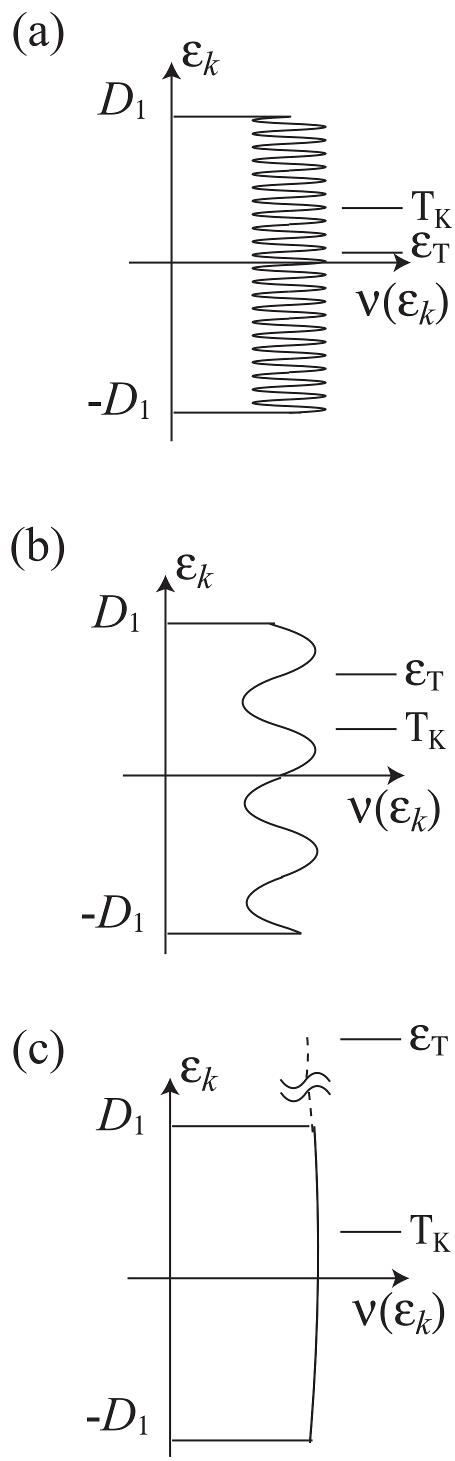

Figure 2 Schematic drawing of the density of states in the lead for the reduced model, in situations (a) $L_c \ll L_K \ll L$, (b) $L_c \ll L \ll L_K$, and (c) $L \ll L_c \ll L_K$, where L is the size of the AB ring, L_c is the screening length of charge fluctuation, and L_K is that of spin fluctuation, i.e., size of Kondo screening cloud. The half of band width is $D_1 \simeq |\varepsilon_0|$ in the second stage of scaling. In situation (a), $\varepsilon_T \ll T_K \ll |\varepsilon_0|$. The oscillating part of $\nu(\varepsilon_k)$ is averaged out in the integration of scaling equations. In consequence, the Kondo temperature T_K does not depend on the ring size nor AB phase φ of the magnetic flux penetrating the ring. In situation (b), $T_K \ll \varepsilon_T \ll |\varepsilon_0|$. Then the Thouless energy ε_T acts as the high energy cut off. φ-dependence of T_K is determined by the ratio of ε_T to T_K. In situation (c), $T_K \ll |\varepsilon_0| \ll \varepsilon_T$. The density of states is almost constant. In this case, T_K reflects the density of states at the Fermi level, $\nu(0)$.

where $f(\varphi) = [1 - f(k_F L + \pi/2, \varphi)]^{-1}$.

In situation (ii), $T_K \ll \varepsilon_T \ll D_1$. The coupling constants, J and K, are renormalized following Equations 17 and 18 when D is reduced from D_1 to ε_T and following Equations 19 and 20 when D is reduced from ε_T to T_K. We match the solutions of the respective equations around $D = \varepsilon_T$ and obtain

$$T_K(\phi) \simeq \varepsilon_T e^{\gamma} \left(T_K^{(0)} \Big/ \varepsilon_T e^{\gamma} \right)^{f(\phi)}, \tag{24}$$

where $\gamma \approx 0.57721$ is the Euler constant.

The different expressions of $T_K(\varphi)$ in the three situations can be explained intuitively. In situation (i), $\varepsilon_T \ll T_K$. Then the oscillating part of the density of states $\nu(\varepsilon_k)$ with period ε_T is averaged out in the scaling procedure (Figure 2a). As a result, the magnetic-flux dependence of T_K disappears. In situation (iii), $T_K \ll \varepsilon_T$. Then $\nu(\varepsilon_k)$ is almost constant in the scaling (Figure 2c). The Kondo temperature significantly depends on the magnetic flux through the constant value of $\nu(0)$ at the Fermi level.

Conclusions

We have theoretically studied the Kondo effect in a quantum dot embedded in an AB ring. The two-stage scaling method yields an analytical expression of the Kondo temperature T_K as a function of AB phase φ of the magnetic flux penetrating the ring. We have obtained different expressions of $T_K(\varphi)$ for (i) $L_c \ll L_K \ll L$, (ii) $L_c \ll L \ll L_K$, and (iii) $L \ll L_c \ll L_K$, where L is the size of the ring, $L_c = \hbar v_F/|\tilde{\varepsilon}_0|$ is the screening length of the charge fluctuation, and $L_K = \hbar v_F/T_K$ is the screening length of the charge fluctuation, i.e., size of Kondo screening cloud. T_K strongly depends on φ in cases (ii) and (iii), whereas it hardly depends on φ in case (i).

Abbreviation

AB: Aharonov-Bohm.

Acknowledgements

This study was partly supported by a Grant-in-Aid for Scientific Research from the Japan Society for the Promotion of Science, and by Global COE Program "High-Level Global Cooperation for Leading-Edge Platform on Access Space (C12)."

Authors' contributions

All authors read and approved the final manuscript.

Competing interests

The authors declare that they have no competing interests.

Received: 3 September 2010 Accepted: 23 November 2011
Published: 23 November 2011

References

1. Goldhaber-Gordon D, Shtrikman H, Mahalu D, Abusch-Magder D, Meirav U, Kastner MA: Kondo effect in a single-electron transistor. *Nature* 1998, **391**:156.
2. Cronenwett SM, Oosterkamp TH, Kouwenhoven LP: A tunable Kondo effect in quantum dots. *Science* 1998, **281**:540.
3. van der Wiel WG, De Franceschi S, Fujisawa T, Elzerman JM, Tarucha S, Kouwenhoven LP: *Science* 2000, **289**:2105.
4. Sasaki S, De Franceschi S, Elzerman JM, van der Wiel WG, Eto M, Tarucha S, Kouwenhoven LP: Kondo effect in an integer-spin quantum dot. *Nature* 2000, **405**:764.
5. Sasaki S, Amaha S, Asakawa N, Eto M, Tarucha S: Enhanced Kondo effect via tuned orbital degeneracy in a spin 1/2 artificial atom. *Phys Rev Lett* 2004, **93**:17205.
6. Aono T, Eto M, Kawamura K: Conductance through quantum dot dimer below the Kondo temperature. *J Phys Soc Jpn* 1998, **67**:1860.
7. Jeong H, Chang AM, Melloch MR: The Kondo effect in an artificial quantum dot molecule. *Science* 2001, **293**:2221.
8. Affleck I, Simon P: Detecting the Kondo screening cloud around a quantum dot. *it Phys Rev Lett* 2001, **86**:432.
9. Affleck I, Borda L, Saleur H: Friedel oscillations and the Kondo screening cloud. *Phys Rev B* 2008, **77**:180404(R).
10. Borda L: Kondo screening cloud in a one-dimensional wire: Numerical renormalization group study. *Phys Rev B* 2008, **75**:041307(R).
11. Holzner A, McCulloch I, Schollwock U, Delft J, Heidrich-Meisner F: Kondo screening cloud in the single-impurity Anderson model: A density matrix renormalization group study. *Phys Rev B* 2009, **80**:205114.
12. Bulka BR, Stefański P: Fano and Kondo resonance in electronic current through nanodevices. *Phys Rev Lett* 2001, **86**:5128.
13. Hofstetter W, König J, Schoeller H: Kondo Correlations and the Fano Effect in Closed Aharonov-Bohm Interferometers. *Phys Rev Lett* 2001, **87**:156803.
14. Konik RM: Kondo-Fano resonances in quantum dots; results from the Bethe ansatz. *J Stat Mech: Theor Exp* 2004, **2004**:L11001.
15. Maruyama I, Shibata N, Ueda K: Theory of Fano-Kondo effect of transport properties through quantum dots. *J Phys Soc Jpn* 2004, **73**:3239.
16. Katsumoto S, Aikawa H, Eto M, Iye Y: Tunable Fano]Kondo effect in a quantum dot with an Aharonov]Bohmring. *Phys Status Solidi C* 2006, **3**:4208.
17. Simon P, Affleck I: Finite-size effects in conductance measurements on quantum dots. *Phys Rev Lett* 2002, **89**:206602.
18. Simon P, Entin-Wohlman O, Aharony A: Flux-dependent Kondo temperature in an Aharonov-Bohm interferometer with an in-line quantum dot. *Phys Rev B* 2005, **72**:245313.
19. Yoshii R, Eto M: Scaling Analysis for Kondo Effect in Quantum Dot Embedded in Aharonov-Bohm Ring. *J Phys Soc Jpn* 2008, **77**:123714.
20. Anderson PW: A poor man's derivation of scaling laws for the Kondo problem. *J Phys C* 1970, **3**:2439.
21. Haldane FDM: Scaling theory of the asymmetric Anderson model. *Phys Rev Lett* 1978, **40**:416.
22. Yoshii R, Eto M: Scaling analysis of Kondo screening cloud in a mesoscopic ring with an embedded quantum dot. *Phys Rev B* 2011, **83**:165310.
23. Eto M: Enhancement of Kondo Effect in Multilevel Quantum Dots. *J Phys Soc Jpn* 2005, **74**:95.

doi:10.1186/1556-276X-6-604
Cite this article as: Yoshii and Eto: Analytical expression of Kondo temperature in quantum dot embedded in Aharonov-Bohm ring. *Nanoscale Research Letters* 2011 **6**:604.